USING THE NOSE-TO-NOSE SAMPLER CALIBRATION METHOD IN PULSE METROLOGY

D.R. Larson[1,], N.G. Paulter[2,*]*

(1) Electricity Division, National Institute of Standards and Technology, Gaithersburg, MD 20899 USA
Phone (301) 975-2437 Fax (301) 926-3972 e-mail: donald.larson@nist.gov
(2) Electricity Division, National Institute of Standards and Technology, Gaithersburg, MD 20899 USA
Phone (301)975-2405 Fax (301) 926-3972 e-mail: nicholas.paulter@nist.gov

Abstract - We present our analysis of the nose-to-nose (ntn) method for use as an accurate sampler calibration method. The variations in the measurement of the sampler impulse response using the ntn method are described and the assertion that the kick-out pulse is identical to the sampler impulse response is assessed. Temperature effects on the ntn method are also examined. Finally, the effect of uncertainties in the ntn calibration method on the uncertainties in reported pulse parameters is examined.

Keywords - sampler calibration, nose-to-nose, kick-out pulse, offset voltage

1. INTRODUCTION

There presently are no widely accepted methods for calibrating the impulse response or complex transfer function of high-bandwidth samplers used in oscilloscopes and network analyzers. Although calibration methods can be performed with either time- or frequency-domain techniques, time-domain techniques are usually preferred because of the difficulty in obtaining phase information from most frequency-domain methods. However, these time-domain methods require pulse generators that have significantly greater bandwidth than the samplers themselves or, if the generators have comparable bandwidth, then their pulse profiles must be accurately known so that the influence of the pulse generator on the measured step response can be deconvolved. A proposed sampler calibration method where both the sampler and pulse generator functions are claimed to be identifiable is the “nose-to-nose” (ntn) method. The ntn method was introduced about 10 years ago, and is a method where a sampler is also used as a pulse generator. In the ntn method, the sampler generates a pulse (termed the “kick-out” pulse) when it is operated at a non-zero offset voltage ($V_{off} \neq 0$ V) and it is argued that the kick-out pulse represents the impulse response of the sampler [1-3]. The generation of a kick-out pulse is limited to a particular type of sampler architecture and not all commercially-available samplers will generate a kick-out pulse.

2. MEASUREMENT

2.1 Description

The nose-to-nose method gets its name from the arrangement of the samplers in the measurement procedure (see Fig. 1) where the input connectors of two different sampling heads are connected together using a male-to-male coaxial adapter. In the ntn technique, three samplers [2] are used, each acting in turn as a sampler and as a source for the kick-out pulse. Kick-out pulses are produced when the sampling structure (a diode bridge) is strobed while under bias (the offset voltage). The offset voltage is the voltage generated internally by the oscilloscope using the "offset voltage" setting of the vertical axis of the oscilloscope. The amplitude of the kick-out pulse is dependent on the offset voltage. The kick-out pulses propagate to the input terminal of the sampler. The measurement procedure we use to investigate the ntn method is described in [4]. In practice, three samplers are used, in all

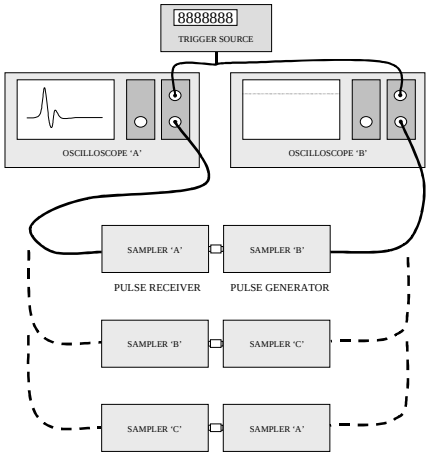

Fig. 1 - Nose-to-nose measurement setup.

[*] Electricity Division, Electronics and Electrical Engineering Laboratory, Technology Administration, Department of Commerce. Official contribution of the National Institute of Standards and Technology, not subject to copyright in the U.S.A.

ISBN 972-98115-4-7 © 2001 IT

permutations of two.

The acquired kick-out waveform, $W(V_{off},t)$, also contains a signal contribution from the sampling-diode strobe pulse, that is

$$W(V_{off},t) = s(V_{off},t) + k(V_{off},t), \qquad (1)$$

where $s(V_{off},t)$ is the coupled strobe pulse and $k(V_{off},t)$ is the kick-out pulse, both taken at the offset voltage V_{off}. The polarity of $k(V_{off},t)$ changes sign with the offset voltage whereas the polarity of $s(V_{off},t)$ does not; therefore, the strobe pulse contribution to $W(V_{off},t)$ can be minimized (but not eliminated, as will be shown later). To reduce the strobe pulse contribution, two acquired waveforms are used, one that is obtained with a negative offset voltage, $W(-V_{off},t)$, and another that is obtained with a positive offset voltage of equal magnitude, $W(+V_{off},t)$. The $k(V_{off},t)$ is approximated by the difference, $D(V_{off},t)$, between $W(-V_{off},t)$ and $W(+V_{off},t)$, where the amplitude is divided by two for proper scaling [2]:

$$D(V_{off},t) = \frac{W(+V_{off},t) - W(-V_{off},t)}{2}. \qquad (2)$$

$D(V_{off},t)$ will equal $k(V_{off},t)$ only if $k(-V_{off},t) = -k(+V_{off},t)$ and $s(-V_{off},t) = s(+V_{off},t)$. For example, the pulse durations of the difference waveforms we have obtained using 50 GHz samplers are approximately 11 ps (full duration at half maximum); however, the waveforms exhibit significant aberrations.

The ntn method requires that both samplers are being strobed. However, one sampler is acting as an impulse generator and the other as a sampling aperture (receiver). The different samplers have associated with them different time-bases, namely, that of their respective mainframes. Whether acting as a pulse generator or a receiver, the sampler is strobed by a fast transition duration step-like pulse (the strobe pulse). This strobe pulse is generated by the timebase after receiving an external trigger signal. In the ntn method, both oscilloscopes use a common trigger source. Jitter will occur between the external trigger pulse and the strobe pulse, and between the strobe pulse and the switching of the sampling diodes. The resultant measured waveforms, $W(V_{off},t)$, from which $D(V_{off},t)$ is obtained, includes the convolution of all these functions:

$$W_{1-2}(V_{off},t) = f_{1,g}(t)*j_{1,g}(t)*f_{2,s}(t)*j_{2,s}(t),$$
$$W_{2-1}(V_{off},t) = f_{2,g}(t)*j_{2,g}(t)*f_{1,s}(t)*j_{1,s}(t),$$

where the subscript "1" and "2" denotes a given sampler, the subscript "g" or "s" denotes whether the sampler is being operated as an impulse generator or a sampling aperture, and the "*" denotes a convolution. For our measurements, the timebase does not change between generator and aperture functions, so the "g" and "s" subscripts on $j(t)$ can be dropped. Consequently, the effect of jitter on $W(V_{off},t)$ does not change when the function of the samplers is changed.

The effect of drift in the timebase will also affect $W(V_{off},t)$. For the measurements we perform, which take less than 3 minutes for each $W(V_{off},t)$, the drift is a slow unidirectional displacement of the signal. This can be viewed as jitter having a uniform distribution. As with jitter, drift is caused by the timebase of the mainframe. And, as with jitter, the effect of drift on $W(V_{off},t)$ does not change when the function of the samplers is changed. Furthermore, if we assume that drift is nominally linear during a given waveform acquisition (worst case) and approximate the drift to be less than 2 ps/ 45 min [5], then for 3 minute waveform acquisitions the drift will be less than 0.14 ps. Furthermore, we have observed no change in the transition duration of step-like waveforms when the number of averages was varied from 32 to 2048 [4] and the variation in these transition duration values equaled the measurement repeatability variation of 0.12 ps (see Sec. 3.1). However, if methods of acquiring the waveforms requires longer times, it may be necessary to correct the waveforms for drift [6].

We have not corrected for non-equispaced sampling intervals (nesi) (also called time-base errors, time-base distortion, time-base nonlinearity) and the spectra shown in Fig. 2 (discussed in Sec. 3.2) may suffer from this. However, we are concerned with the transition duration of the reconstructed waveforms. Uncertainties in these transition durations is based on having estimates for variations in the transition duration of the sampler step response and an empirical relationship [7] we have developed that relates the transition duration of the reconstructed waveform to that of sampler step-response. In our measurement process, we position the transition region of all of the $W(V_{off},t)$ so they occur in nominally the same region of the waveform epoch and this region exhibits a nominally monotonic time-base error, that is, an error that can be fit by a straight line. We have observed

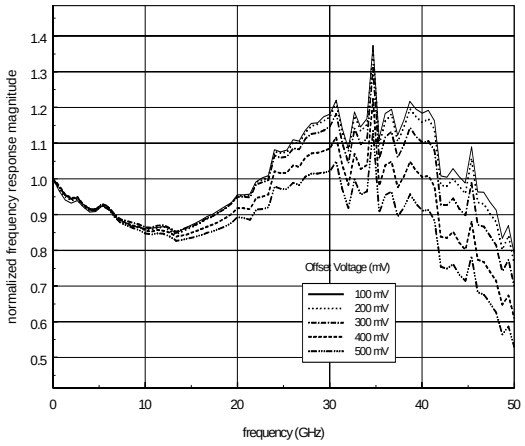

Fig.2 - Magnitude spectra of acquired waveforms, $D(V_{off},t)$, for offset voltages of 100 mV, 200 mV, 300 mV, 400 mV, and 500 mV normalized to the magnitude of their corresponding dc components.

that the nesi for the time-bases used in the ntn method is stationary [4]. Local expansion or contraction of the time-base sampling intervals is measured [8] and the transition duration values are adjusted accordingly.

3. MEASUREMENT RESULTS

3.1 Measurement repeatability

An important contributor to uncertainties in sampler calibration may be the repeatability of the ntn measurements. To examine this possibility, two sets of five $D(V_{off},t)$ were acquired, one set without connecting and disconnecting the two samplers between measurements and one set with connecting and disconnecting the samplers, and their step parameters compared. For the set without disconnections, the 10 % to 90 % transition duration, $t_{10\text{-}90}$, was observed to be 13.11 ps ± 0.12 ps, and the pulse amplitude was 0.440 V ± 0.005 V. For the set with disconnections between measurements, the observed $t_{10\text{-}90}$ was 12.94 ps ± 0.30 ps and the amplitude was 0.435 V ± 0.003 V. The variation in the $t_{10\text{-}90}$ values for the set of waveforms obtained after disconnecting and reconnecting the samplers also includes the measurement repeatability variation. From these data, it can be seen that connecting and disconnecting the two samplers affects both the pulse amplitude and the $t_{10\text{-}90}$ average values and the uncertainty in $t_{10\text{-}90}$. However, since it is not necessary to disconnect the two samplers when acquiring a set of $D(V_{off},t)$ from which an estimate of the sampler impulse response is obtained, a smaller uncertainty effect on $t_{10\text{-}90}$ can be ascribed to measurement repeatability.

3.2 Temperature effects

The changes in the 20 % to 80 % transition durations ($t_{20\text{-}80}$) and pulse amplitudes of a measured pulse as a function of the sampling head temperature [9] are shown in Table 1. The measurement process and conditions are reported in [9]. The values for pulse amplitude and $t_{20\text{-}80}$ for the samplers acting as either a pulse transmitter (denoted by "T") or receiver (denoted by "R") are listed in Table 1.

Table 1 - Temperature coefficients of pulse parameters.

	amplitude slope (mV/°C)	$t_{20\text{-}80}$ slope (ps/°C)
R1, 50 GHz	-1.478	-0.003
R2, 20 GHz	0.093	0.041
T1, 50 GHz	-1.423	-0.01

3.3 Nonlinear V_{off}-dependence of kick-out pulse

The Fourier transforms of the difference waveforms were calculated to examine the effect of V_{off} on the spectra of $D(V_{off},t)$. Fig. 2 shows the spectra of $D(V_{off},t)$ for various offset voltages and normalized to the magnitude of their corresponding dc components. Fig. 2 shows that the normalized magnitude spectra of the $D(V_{off},t)$ are dependent on V_{off}. The maximum random (Type A) amplitude uncertainty for all frequency components of the spectrum of $D(V_{off},t)$ is 2.2 %. It should be noted that $W(-V_{off},t)$ and $W(+V_{off},t)$ and, consequently, $D(V_{off},t)$ are the result of the convolution of the $k(V_{off},t)$ and $s(V_{off},t)$ with the impulse response of the sampler-to-sampler adapter and the impulse response of the measuring sampler. Accordingly, the spectra shown in Fig. 2 reflect this convolution. However, the plots shown in Fig. 2 can be used to estimate the -3 dB attenuation bandwidths of the $D(V_{off},t)$ as a function of V_{off}. An approximate correction for the convolution process is to take the square root of the spectrum. Doing this correction, the bandwidth can be seen to decrease slightly with increasing offset voltage up to around ± 300 mV (see Fig. 3). For offset voltages outside this range, the decrease in bandwidth becomes more significant. The -3 dB frequency decreases from approximately 50.3 GHz at V_{off} = ± 200 mV to approximately 45.8 GHz at V_{off} = ± 500 mV.

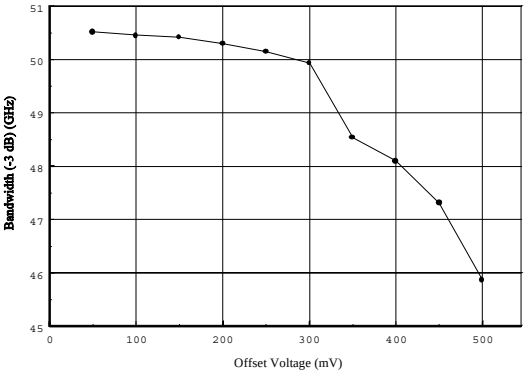

Fig. 3 - The -3 dB attenuation frequency of the spectra of $D(V_{off},t)$ as a function of V_{off}.

3.4 V_{off}-dependence of strobe pulse coupling [10]

The strobe pulse contribution to the kick-out pulse can be approximated using:

$$G(V_{off},t) = \frac{W(+V_{off},t) + W(-V_{off},t)}{2}. \qquad (3)$$

Several $s(V_{off},t)$ were computed using (3) and their magnitude spectra are shown in Fig. 4. This figure shows the dependence of strobe pulse coupling on offset voltage. For frequencies greater than about 15 GHz, the difference in the spectra of the $G(V_{off},t)$ is large. There also appears to be an anomaly near the offset voltage setting of 400 mV.

3.5 Strobe pulse coupling and harmonic distortion

The coupling of the strobe pulse was also measured by

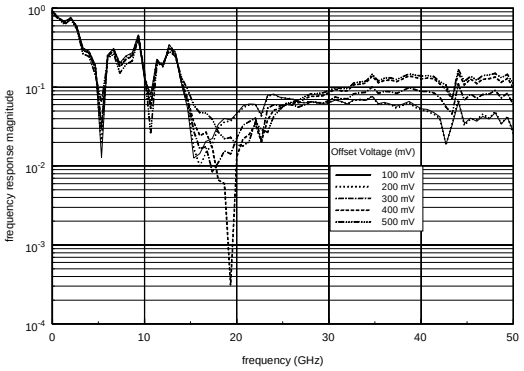

Fig. 4 - Magnitude of the spectrum of $G(V_{off},t)$.

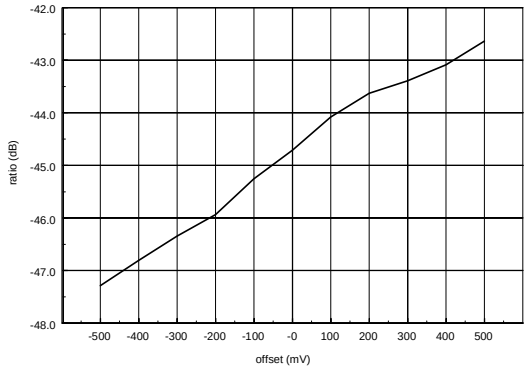

Fig. 5 - Harmonic distortion of a 20 GHz sinewave as a function of V_{off}. The ratio is that of the amplitude of the second harmonic to the amplitude of the first harmonic.

acquiring the waveform of a nominally spectrally-pure sinusoidal signal generated by a synthesized frequency source. The offset voltage was varied and the signal amplitude was kept constant for these measurements. To determine if strobe coupling affected the sampling process alone, that is, without the influence of a kick-out pulse, a fixed frequency (20 GHz, manufacturer specification for spectral purity is -55 dBc.) 150 mV peak-to-peak sinewave was measured. The offset voltage of the sampler was varied from -500 mV to 500 mV in 100 mV steps. To ensure that the measured sinewave spanned the same range of the sampler analog-to-digital converter (ADC) for each V_{off}, a constant voltage signal (equal to V_{off}) was added to the input of the sampler through a bias tee. The first ten harmonics of the sinusoidal waveform as a function of V_{off} were examined. Only the second harmonic of 20 GHz exhibited any observable dependence on V_{off}. The third harmonic contained more energy than the second harmonic but did not display any dependence on V_{off}. Fig. 5 shows that the sampling process itself is affected by V_{off}. Consequently, V_{off} of the receiving sampler in the ntn method should be set to 0 V. This effect will also impact pulse metrology in situations where the signal must be offset to record it.

3.6 Validity of ntn assertion

A direct measurement of the assertion that the kick-out pulse and sampling aperture are equivalent was performed. In this comparison, two sets of $W(V_{off},t)$ are obtained. In the first set, $W(V_{off},t)$ is obtained using sampler 1 (S1) as the receiver (or measuring device) and sampler 2 (S2) as the transmitter (or pulse generator). In the second set, S1 is used as the transmitter and S2 as the receiver. This was done for offset voltages of -175 mV and 175 mV. The difference between the waveforms $W_{1\text{-}2}(V_{off},t)$ and $W_{2\text{-}1}(V_{off},t)$ for each offset voltage is shown in Fig. 6. This figure shows that the ntn assertion is not exact, that is, the samplers behave differently when acting as a sampler or a pulse generator.

4. UNCERTAINTY CONSIDERATIONS

To determine the applicability of the ntn method to sampler calibration, the magnitude of the effect of uncertainties from the ntn calibration method on the uncertainties of the pulse parameters of a measured pulse is considered. Actually, it is not the measured pulse for which pulse parameters are calculated, but the reconstructed waveform that is the best estimate to the measured (or input) pulse. The reconstructed waveform is obtained after deconvolving the sampler impulse response from the measured pulse's waveform. An uncertainty analysis has been developed where empirical equations are used to obtain the uncertainty in pulse parameters of the reconstructed waveform as a function of the uncertainties in the impulse response estimate[7,11]. In particular, these equations relate the pulse parameters of the reconstructed waveform to the pulse parameters of the impulse response estimate and the

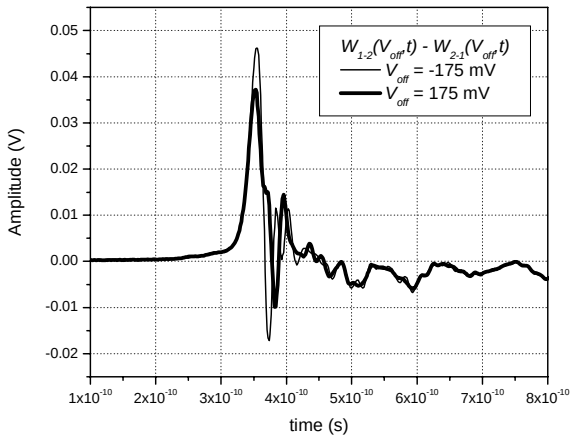

Fig. 6 - Difference of kick-out waveforms using two samplers where the receiving and transmitting functions of the samplers have been interchanged. The two plots are for V_{off} = 175 mV and V_{off} = -175 mV.

acquired waveform. Using these equations we can assess the importance of uncertainties in the ntn calibration method to the uncertainties in pulse parameters we report to our customers.

The effects of temperature on the sampling heads, acting as a pulse generator or measuring device, are relatively small for the observed temperature variations during measurement (< 0.6 °C). The effects of measurement repeatability (causing a variation in $t_{10\text{-}90}$ of 0.12 ps) and disconnecting and reconnecting the samplers (causing a variation in $t_{10\text{-}90}$ of 0.27 ps) causes a total variation in the $t_{10\text{-}90}$ of the measured waveform of approximately 0.30 ps; these effects on calibration uncertainty must be considered.

To get an approximation for the magnitude of the uncertainties in $t_{10\text{-}90}$ caused by the ntn assertion error, the variation in the $t_{10\text{-}90}$ of ten difference waveforms was computed. The difference waveforms were acquired without disconnecting the samplers, five with S1 acting as the receiver and S2 as the transmitter, and five with S2 acting as the receiver and S1 as the transmitter. From the variation in these measurements, we estimate the uncertainty in transition duration to be approximately 0.21 ps (the 0.12 ps repeatability contribution has been removed). This 0.21 ps uncertainty value is for one pair of samplers whereas in the ntn method three pairs of samplers are required, therefore, the total ntn $t_{10\text{-}90}$ uncertainty is approximately 0.36 ps (assuming the uncertainties for all pairs is normally distributed). It should be noted that the difference in $t_{10\text{-}90}$ between the average of the S1/S2 set and the average of the S2/S1 set was 0.35 ps, indicating that the samplers do not behave identically when acting as a transmitter or a receiver. From our empirical equation, we estimate that the ntn assertion error corresponds to an uncertainty in the reconstructed waveform $t_{r,10\text{-}90}$ of approximately ± 1.23 ps (for nine degrees of freedom and a confidence interval of 95.45 %, that is, 2σ). This uncertainty value is approximated using a measured waveform $t_{m,10\text{-}90}$ of 12.2 ps and a simulated system response $t_{s,10\text{-}90}$ of approximately 10 ps. If $t_{s,10\text{-}90}$ increases or $t_{m,10\text{-}90}$ decreases, the uncertainty in $t_{r,10\text{-}90}$ increases. The additional effect of measurement repeatability increases this 2σ uncertainty to ± 1.29 ps. If the effect of sampler connect/disconnect is included, which is necessary using the three sampler ntn method [4], the 2σ uncertainty is ± 1.61 ps. The 2σ uncertainty for the transition duration of the sampler step response was about ± 1.2 ps.

5. SUMMARY

The spectra of the difference waveforms (see Fig. 2) and the variation in -3 dB attenuation bandwidth (see Fig. 3) show a dependence on offset voltage and this dependence limits the upper range of useful (for sampler calibration purposes) offset voltage magnitudes to ≤ 200 mV. Furthermore, we have observed (data not shown) that the peak-to-peak amplitude of the kick-out pulses is not linear with offset voltage for offset voltage magnitudes ≤ 100 mV[4], which puts a lower limit on the offset voltage. Measurement repeatability and temperature effects have a small effect on the uncertainties in the reported pulse parameters. However, the ntn sampler calibration method will cause large uncertainties in the reported transition duration values of short-transition-duration pulses. For example, for a pulse with a nominal $t_{10\text{-}90}$ of less than 7 ps, a 1.61 ps uncertainty is significant. To make the three-sampler ntn sampler calibration method useful for accurate measurements ($t_{10\text{-}90}$ uncertainties less than 5 %) of short-$t_{10\text{-}90}$ pulses will require that the samplers behave more similarly than they presently do. Although we have only shown the effect of errors in the ntn method on transition duration, the differences shown in Fig. 6 will cause errors in the determinations of waveform aberrations, including overshoot, undershoot (preshoot), and settling time. However, since the accuracy of other sampler calibration methods has not been determined, the ntn method is a reasonable calibration technique to use. Furthermore, for routine (non-metrological) purposes, the three-sampler ntn method is adequate.

ACKNOWLEDGMENTS

The authors would like to thank P.D. Hale of the National Institute of Standards and Technology (NIST), Boulder, CO and T.M. Souders, retired, NIST, Gaithersburg, MD for technical comments on this paper and B.A. Bell of the NIST, Gaithersburg, MD for administrative support.

REFERENCES

[1] K. Rush, S. Draving, and J. Kerley, "Characterizing high-speed oscilloscopes," IEEE Spectrum, September 1990, pp. 38 to 39.

[2] J. Verspecht, "Broadband sampling oscilloscope characterization with the 'nose-to-nose' calibration procedure: A theoretical and practical analysis," IEEE Trans. Instrum. Meas., Vol. 44, December 1995, pp. 991 to 997.

[3] J. Verspecht, "Accurate spectral estimation based on measurements with a distorted-timebase digitizer," IEEE Trans. Instrum. Meas., Vol. 43, April 1994, pp. 210 to 215.

[4] D.R. Larson and N.G. Paulter, "The effects of offset voltage on the kick-out pulses used in the nose-to-nose sampler impulse response characterization method," Instrumentation and Measurement Technology Conference, IMTC 2000, Baltimore, USA, May 2000, pp. 1425 to 1428.

[5] P.D. Hale, T.S. Clement, K.J. Coakley, C.M. Wang, D.C. DeGroot, and A.P. Verdoni, "Estimating the magnitude and phase response of a 50 GHz sampling oscilloscope using the 'nose-to-nose' method," Automatic Radio Frequency Technology Group, 55th ARFTG Conference, Boston, USA, June 2000.

[6] K.J. Coakley and P.D. Hale, "Alignment of Noisy Signals," IEEE Trans. Instrum. Meas., Vol. 50, 2001, pp. 141 to 149.

[7] N.G. Paulter and D.R. Larson, "Improving the Uncertainty Analysis of NIST's Pulse Parameter Measurement Service," 56th ARFTG Conference Digest, Boulder, CO, USA, 30 November and 1 December 2000, pp. 16 to 24.

[8] G.N. Stenbakken and J.P. Deyst, "Time-base nonlinearity determination using iterated sine-fit analysis," IEEE Trans. Instrum. Meas., Vol. 47, 1998, pp. 1056 to 1061.

[9] D.R. Larson and N.G. Paulter, "Temperature effects on the high speed response of digitizing sampling oscilloscopes," NCSL International, 2000 Workshop and Symposium, Toronto, Canada, July 2000.

[10] N.G. Paulter and D.R. Larson, "An Examination of the Spectra of the "Kick-out" Pulses for a Proposed Sampling Oscilloscope Calibration Method," accepted for publication IEEE Trans. Instrum. Meas.

[11] N.G. Paulter and D.R. Larson, " An Uncertainty Analysis of the High-speed Pulse Parameter Measurements at NIST," IMEKO TC-4 Symposium and ADC Workshop, Lisbon, Portugal, 13 - 14 September 2001.